Observational constraints on a Unified Dark Matter model with fast transition

ALBERTO ROZAS-FERNÁNDEZ (in collaboration with Diogo Castelão and Ismael Tereno)

(IA, University of Lisbon)

VII MFC, Madrid, 9 September

Introduction

- Unified Dark Matter (UDM): a single matter component explains both structure formation and cosmic acceleration
- UDM are appealing because evade the coincidence problem and predict $w_{DE} \approx -1$
- Appearance of $c_s^2 \neq 0$ (non-negligible Jeans scale/strong late ISW effect)
- Possible solution: UDM models with fast transition between an early CDM-like phase and a late ΛCDM-like epoch
- Our aim: study the observational viability at structure formation level of a UDM model with fast transition

The model

The energy density of this UDM model (see M. Bruni al, MNRAS 431 (2013) 2907-2916) is given by

$$\rho = \begin{cases} \rho_t \left(\frac{a_t}{a}\right)^3 & a < a_t \\ \rho_\Lambda + (\rho_t - \rho_\Lambda) \left(\frac{a_t}{a}\right)^3 & a > a_t \end{cases} \quad (1)$$

where a_t represents the value of the scale factor at the transition and β refers to the rapidity of the transition. In addition to a_t and β, there is a third parameter in this model, ρ_Λ (or equivalently Ω_Λ), that plays the role of an effective cosmological constant.

The model

It is useful to explicitly incorporate a Heaviside function $H(a - a_{\rm t})$ so that

$$\rho = \rho_{\rm t} \left(\frac{a_{\rm t}}{a}\right)^3 + \rho_\Lambda \left[1 - \left(\frac{a_{\rm t}}{a}\right)^3\right] H(a - a_{\rm t}) \ , \tag{2}$$

We shall use the following continuous approximation to the Heaviside function

$$H_{\rm t}(a - a_{\rm t}) = \frac{1}{2} + \frac{1}{\pi} \arctan(\beta(a - a_{\rm t})), \tag{3}$$

Conditions for viability of UDM models

- Any viable UDM model should satisfy the condition $k_{\mathrm{J}}^2 \gg k^2$ for all the scales of cosmological interest
- The explicit form of the Jeans wave number is

$$k_{\mathrm{J}}^2 = \frac{3}{2}\rho a^2 \frac{(1+w)}{c_{\mathrm{s}}^2} \left| \frac{1}{2}(c_{\mathrm{s}}^2 - w) - \rho \frac{dc_{\mathrm{s}}^2}{d\rho} + \frac{3(c_{\mathrm{s}}^2 - w)^2 - 2(c_{\mathrm{s}}^2 - w)}{6(1+w)} + \frac{1}{3} \right| . \quad (4)$$

- We can obtain a large k_{J}^2 when we have $c_s^2 = 0$ but also when c_s^2 changes rapidly. This is the motivation to build UDM models with fast transition.

Speed of sound in fast transition models

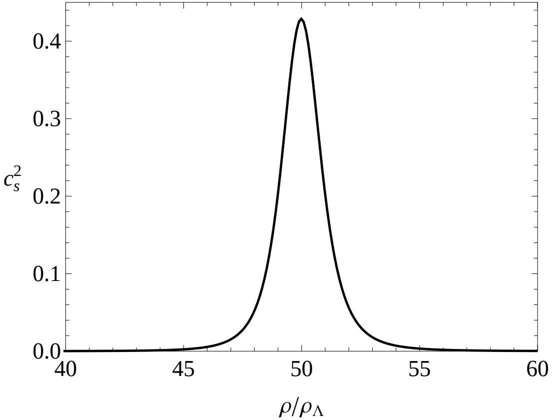

- The amplitude depends on a_t and β. Faster transitions produce higher and narrower peaks. Earlier transitions for equal rapidities produce peaks with smaller areas.

Matter power spectra for different a_t and β

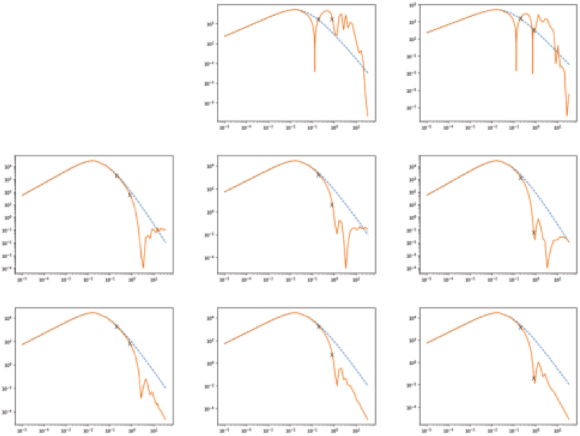

Figure: Dependence of the matter power spectrum on a_t and β. a_t increases from bottom to top and β increases from right to left, while $\Omega_{\Lambda udm}$ is kept fixed at 0.7. The crosses show the effective scales of the structure formation data used in our analyses

KiDS data points used

- When including KiDS data, in principle we need to consider the non-linear matter power spectrum. The problem is that when there are oscillations in it, we cannot apply a non-linear correction (HALOFIT).
- We found that $k = 0.28 - 0.84$ is the widest range of the matter power spectrum probed by the KiDS lensing power spectra. These two data points are then in the mildly non-linear regime, since the threshold is usually considered to be $k = 0.2\,\mathrm{h/Mpc}$.
- We computed the matter power spectrum for ΛCDM model with and without HALOFIT. The linear and non-linear power spectra are identical for large scales ($k < 0.2\,\mathrm{h/Mpc}$) and deviate for smaller scales. We then computed the likelihood of these ΛCDM power spectra using only these two points in the five KiDS power spectra. We found that the two likelihoods (ΛCDM with and without HALOFIT) deviate by 10%.
- Therefore, we are implicitly introducing an extra theoretical uncertainty of around 10% in the statistical analysis.

MCMC analysis

For several combinations of β, $\Omega_{\Lambda udm}$, and a_t, we find that $c_s^2 > 1$. In fact, for very high β, only a very small region of a_t gives a $c_s^2 \leq 1$ (e.g., $\beta = 500000$ and $\Omega_{\Lambda udm} = 0.72$, only the range $a_t \leq 0.041$ gives $c_s^2 \leq 1$). This means that if we try to run a chain exploring a wide prior for a_t and β at the same time such as $a_t \in [0, 1]$ and $\beta \in [0, 500000]$, a very large amount of points will be rejected, which could be a problem if there is not enough time and computer resources.

	$a_{t,udm}$	β_{udm}	$\Omega_{\Lambda udm}$
regime 1	0.15 - 1	0.01 - 10^3	0.01 - 1
regime 2	0.055 - 0.15	0.01 - $10^{4.5}$	0.01 - 1
regime 3	0.001 - 0.055	0.01 - $10^{5.7}$	0.01 - 1

Table: Ranges for the UDM parameters used in the MCMC runs.

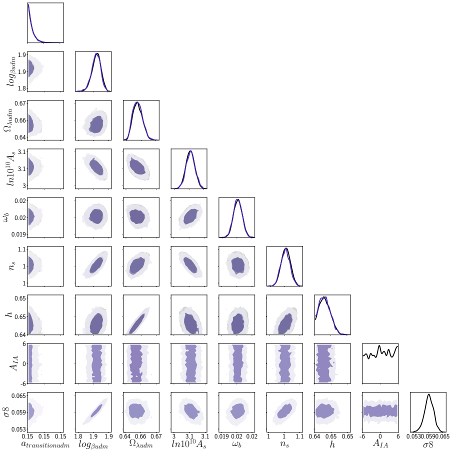

Figure: Regime 1: Posterior probabilities for each parameter in the vanilla set-up, as well as the contours with the 1-σ and 2-σ confidence regions for the analysis with (black lines) and without KiDS (blue lines).

MCMC analysis

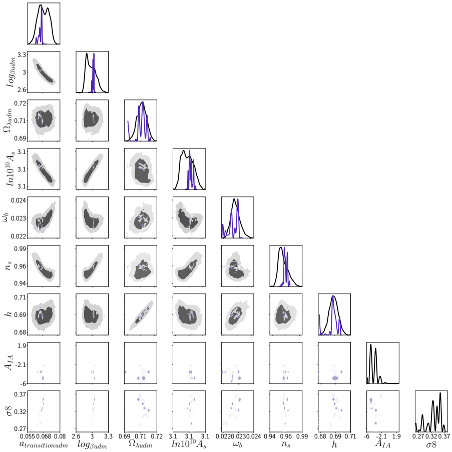

Figure: Regime 2: Posterior probabilities for each parameter in the vanilla set-up, as well as the contours with the 1-σ and 2-σ confidence regions for the analysis with (black lines) and without KiDS (blue lines).

MCMC analysis

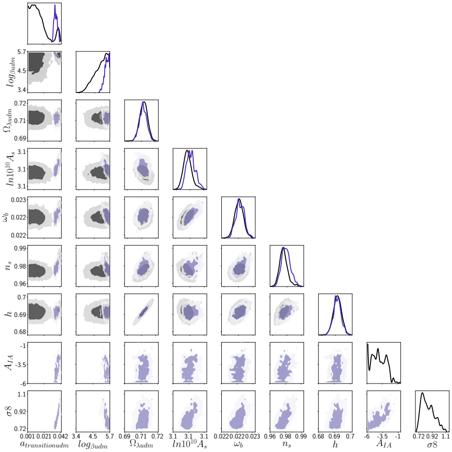

Figure: Regime 3: Posterior probabilities for each parameter in the vanilla set-up, as well as the contours with the 1-σ and 2-σ confidence regions for the analysis with (black lines) and without KiDS (blue lines).

MCMC analysis

Parameters	best-fit	mean$\pm\sigma$	95% lower	95% upper
a_t	0.01182	$0.01616^{+0.0079}_{-0.0119}$	0.00209	0.03052
log_β	5.63	$4.631^{+1.2771}_{-1.3052}$	3.0458	5.6281
$\Omega_{\Lambda udm}$	0.6884	$0.6884^{+0.0008}_{-0.00078}$	0.6868	0.69
$ln10^{10}A_s$	3.121	$3.121^{+0.0019}_{-0.002}$	3.117	3.125

$-\ln\mathcal{L}_{\min} = 5379.71$, minimum $\chi^2 = 1.076e+04$

Table: Estimated best-fit, mean, 1-σ uncertainty and the 2-σ intervals constraints for regime 3 without KiDS data.

MCMC analysis

Parameters	best-fit	mean$\pm\sigma$	95% lower	95% upper
a_t	0.0349	$0.03614^{+0.0016}_{-0.0015}$	0.03312	0.0389
log_β	5.639	$5.568^{+0.13}_{-0.04}$	5.378	5.7
$\Omega_{\Lambda udm}$	0.6886	$0.6883^{+0.00086}_{-0.00075}$	0.6867	0.6899
$ln10^{10}A_s$	3.121	$3.122^{+0.002}_{-0.0021}$	3.118	3.126
A_{IA}	-4.333	$-4.413^{+0.2701}_{-1.4360}$	-5.8489	-2.4071
$\sigma 8$	0.7726	$0.7703^{+0.03}_{-0.047}$	0.6967	0.8559

$-\ln \mathcal{L}_{\min} = 5413.66$, minimum $\chi^2 = 1.083e+04$

Table: Estimated best-fit, mean, 1-σ uncertainty and the 2-σ intervals constraints for regime 3 with KiDS data.

Nested sampling analysis

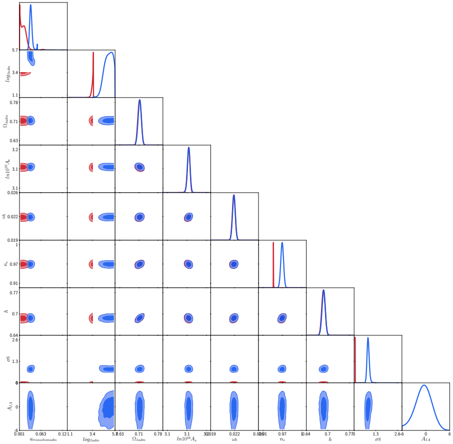

Figure: Posterior probabilities for each parameter in the vanilla set-up, as well as the contours with the 1-σ and 2-σ confidence regions for the analysis with (blue lines) and without KiDS (red lines)

Nested sampling analysis

	a_t	β	$\Omega_{\Lambda udm}$
prior	0.0001 - 0.15	0.01 - $10^{5.7}$	0.01 - 1

Table: The ranges for the UDM parameters used in the nested sampling analysis

Nested sampling analysis

Param	best-fit	mean$\pm\sigma$	95% lower	95% upper
a_t	0.005091	$0.01234^{+0.0028}_{-0.011}$	0.001001	0.0268
log_β	3.498	$3.39^{+0.11}_{-0.033}$	3.169	3.5
$\Omega_{\Lambda udm}$	0.7072	$0.7074^{+0.0072}_{-0.0072}$	0.6936	0.7216
$ln10^{10}A_s$	3.118	$3.118^{+0.0052}_{-0.0041}$	3.108	3.126
ω_b	0.02246	$0.02238^{+0.00026}_{-0.00025}$	0.02187	0.02283
n_s	0.9748	$0.9718^{+0.0054}_{-0.0049}$	0.9607	0.9829
h	0.6908	$0.6907^{+0.0056}_{-0.0058}$	0.6798	0.702
$\sigma 8$	0	$0^{+0.047}_{0.0032}$	-0.01428	0.06428

$$-\ln \mathcal{L}_{\min} = 5374.73, \text{ minimum } \chi^2 = 1.075e+04$$

Table: Estimated best-fit, mean, 1-σ uncertainty and the 2-σ intervals constraints for the nested sampling analysis without KiDS data.

Nested sampling analysis

Param	best-fit	mean$\pm\sigma$	95% lower	95% upper
a_t	0.03092	$0.03309^{+0.0033}_{-0.0048}$	0.02568	0.04235
log_β	5.457	$5.024^{+0.64}_{-0.24}$	4.266	5.699
$\Omega_{\lambda udm}$	0.7086	$0.7082^{+0.0072}_{-0.0066}$	0.694	0.7211
$ln10^{10}A_s$	3.12	$3.118^{+0.0044}_{-0.0047}$	3.11	3.128
ω_b	0.02251	$0.02241^{+0.00025}_{-0.00026}$	0.02196	0.02291
n_s	0.9713	$0.9722^{+0.0056}_{-0.0052}$	0.961	0.9819
h	0.692	$0.6914^{+0.0054}_{-0.0055}$	0.6811	0.703
A_{IA}	0.3906	$-0.5744^{+2.3}_{-1.9}$	-4.944	3.296
$\sigma 8$	0.8616	$0.8551^{+0.064}_{-0.11}$	0.6934	1.04

$-\ln \mathcal{L}_{\min} = 5392.94$, minimum $\chi^2 = 1.079e+04$

Table: Estimated best-fit, mean, 1-σ uncertainty and the 2-σ intervals constraints for the nested sampling analysis with KiDS data.

Model comparison

	ΛCDM	UDM_1	UDM_2	UDM_3	UDM(NS)
χ^2	5394.00	5600.97	5396.25	5406.97	5392.94
χ^2_{red}	0.93048	0.96618	0.93087	0.93272	0.93030
BIC	5445.99	5670.28	5465.56	5476.28	5462.26
DIC	5400.18	5611.19	$--$	5430.04	$--$
AIC	5406.00	5616.97	5412.25	5422.97	5408.94

Table: Values from model comparison criteria, computed for the MCMC and Nested Sampling analyes of the UDM model and for a ΛCDM control analysis.

The nested sampling analysis shows a very good best-fit for the UDM model that is better than the ΛCDM one, even when reduced by the number of degrees-of-freedom. This means that the penalty of having a larger number of extra parameters, does not prevent it from having comparable numbers to ΛCDM in the reduced χ^2, AIC and BIC criteria.

Conclusions

- UDM models have the advantage that they can describe the dynamics of the Universe with a single dark fluid which triggers both the accelerated expansion at late times and the LSS formation at earlier times
- UDM models have no coincidence problem by definition and predict an effective cosmological constant at late times
- We have constrained observationally, at structure formation level, a UDM model with a fast transition between an Einstein de Sitter model, and a more recent epoch whose dynamics, background and perturbative, are that of a standard ΛCDM model.
- We have shown that for an early enough fast transition our UDM model is compatible with observations at background, linear and midly non-linear level and that it is a viable alternative to ΛCDM.
- Next: Spherical collapse and N-body.